Journal of Organometallic Chemistry, 471 (1994) 171–177

The redox behaviour of ferrocene derivatives

VI *. Benzylferrocenes. The crystal structure of decabenzylferrocenium tetrafluoroborate

P. Zanello, A. Cinquantini, S. Mangani and G. Opromolla

Dipartimento di Chimica dell'Università di Siena, Pian dei Mantellini, 44, 53100 Siena (Italy)

L. Pardi

Dipartimento di Chimica dell'Università di Firenze, Via Maragliano 77, 50144 Firenze (Italy)

C. Janiak

Institut für Anorganische und Analytische Chemie der Technischen Universität Berlin, Strasse des 17 Juni 135, D-1000 Berlin 12 (Germany)

M.D. Rausch

Department of Chemistry, University of Massachusetts, Amherst, MA 01003 (USA)

(Received July 14, 1993)

Abstract

The electrochemical behaviour of the benzyl-substituted ferrocenes $[(\eta^5\text{-}C_5Bz_5)_2Fe]$ and $[(\eta^5\text{-}C_5Bz_5)Fe(\eta^5\text{-}C_5H_5)]$ in non-aqueous solutions has been examined. As expected, they undergo reversible one-electron removal more easily than ferrocene itself, but with significantly more difficulty than $[(\eta^5\text{-}C_5R_5)_2Fe]$ (R = Me or Et). In dichloromethane solution, the formal electrode potentials (*vs.* SCE) are as follows: $E^{o\prime}([(C_5Bz_5)_2Fe]^{+/0}) = +0.38$ V, $E^{o\prime}([(C_5Me_5)_2Fe]^{+/0}) = -0.10$ V, $E^{o\prime}([(C_5Et_5)_2Fe]^{+/0}) = -0.06$ V, $E^{o\prime}([(C_5H_5)_2Fe]^{+/0}) = +0.45$ V. The electrochemical properties suggest that the $[(C_5Bz_5)_2Fe]^{+/0}$ redox change should be accompanied by minor, but detectable geometrical strains. In order to define more quantitatively the geometrical reorganization accompanying such electron removal processes, the X-ray structure of $[(C_5Bz_5)_2Fe][BF_4]$ has been determined. Comparison with the previously determined structure of neutral $[(C_5Bz_5)_2Fe]$ shows an elongation of about 0.05 Å of the $Fe\text{–}C_{(cyclopentadienyl)}$ distances, which is a common feature of all ferrocene/ferrocenium couples, but this is also accompanied by reorganization of the peripheral benzyl substituents. In the neutral precursor, the methylene fragments are tilted away from the plane of the cyclopentadienyl rings towards the iron atom, whereas in the monocation they become coplanar.

Key words: Ferrocene; X-ray diffraction; Electrochemistry

1. Introduction

A characteristic of ferrocene molecules is their ability to support the removal of one electron, without decomposition [2]. As far as the decasubstituted ferrocenes $[(\eta^5\text{-}C_5R_5)_2Fe]$ are concerned, the redox properties of the decamethyl [3–8] and decaethyl [9] complexes have been studied. The stereochemical consequences of the removal of one electron are easily discernible for the species with R = Me, in that a large number of X-ray determinations have been performed on the partners of the redox couple $(C_5Me_5)_2Fe$ [10–12]/$[(C_5Me_5)_2Fe]^+$ [13–22]. In contrast, for the species

Correspondence to: Professor P. Zanello, Dr. C. Janiak or Professor M.D. Rausch.

* For Part V, see ref. 1.

0022-328X/94/$7.00
SSDI 0022-328X(93)24227-V

with R = Et, the X-ray structure of only the cation $[(C_5Et_5)_2Fe]^+$ has been reported [9,23].

Recently, two of us independently reported the synthesis and crystal structure of decabenzylferrocene [24,25], and we report here its electrochemical behaviour and the X-ray structure of a salt of the corresponding monocation $[(\eta^5\text{-}C_5Bz_5)_2Fe]^+$.

2. Results and discussion

2.1. Electrochemistry of decabenzylferrocene

Figure 1 shows the cyclic voltammogram of $[(C_5Bz_5)_2Fe]$ in dichloromethane solution.

It undergoes an anodic process, with a directly associated reduction response in the reverse scan. Controlled potential coulometry ($E_w = +0.6$ V) shows that this oxidation step involves one electron/molecule. The exhaustively oxidized solution exhibits a cyclic voltammetric response complementary to that shown in Fig. 1, attesting to the full chemical reversibility of the $[(C_5Bz_5)_2Fe]/[(C_5Bz_5)_2Fe]^+$ redox change.

Upon one-electron oxidation, the yellow solution of $[(C_5Bz_5)_2Fe]$ ($\lambda_{max} = 438$ nm; $\epsilon = 253$ M^{-1} cm^{-1}) grows dark ($\lambda_{max} = 795$ nm; $\epsilon = 1460$ M^{-1} cm^{-1}).

Consistent with the simple one-electron transfer, analysis [26] of the cyclic voltammetric responses with scan rates v varying from 0.02 V s^{-1} to 2.00 V s^{-1} indicates that: (i) the cathodic-to-anodic peak-current ratio, i_{pc}/i_{pa}, is always 1; (ii) the current function $i_{pa} \cdot v^{-1/2}$ remains substantially constant; (iii) the peak-to-peak separation, ΔE_p, progressively increases from 78 mV to 254 mV.

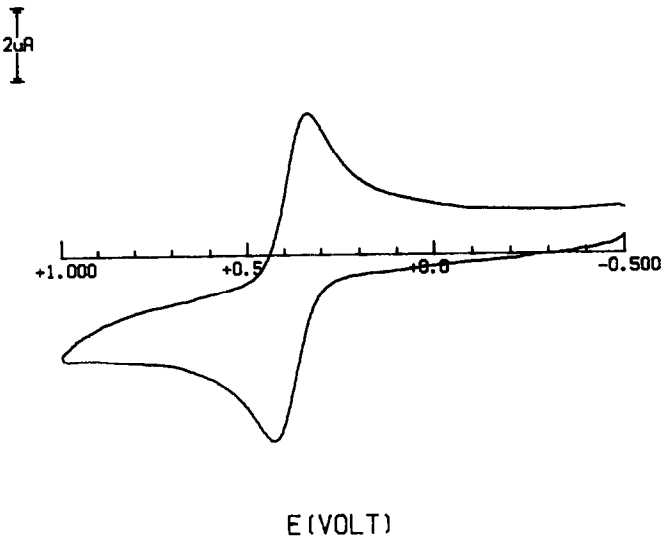

Fig. 1. Cyclic voltammetric response at a platinum electrode of a CH_2Cl_2 solution containing $[(C_5Bz_5)_2Fe]$ (5.4×10^{-4} mol dm^{-3}) and $[NBu_4][ClO_4]$ (0.2 mol dm^{-3}). Scan rate 0.1 V s^{-1}.

TABLE 1. Formal electrode potentials (in volts, *vs.* SCE) and peak-to-peak separation (in mV) for the one-electron oxidation of selected ferrocene molecules in different non-aqueous solutions

Complex	$E°$	ΔE_p [a]	Solvent	Reference
$[(C_5Me_5)_2Fe]$	−0.10	92	CH_2Cl_2 [b]	[c]
	−0.12	79	MeCN [d]	[c]
	+0.13	131	THF [b]	[c]
$[(C_5Et_5)_2Fe]$	−0.06		CH_2Cl_2	9
	−0.06		MeCN	9
$[(C_5Bz_5)_2Fe]$	+0.38	116	CH_2Cl_2 [b]	[c]
	+0.28	98	MeCN [d]	[c]
	+0.51	172	THF [b]	[c]
$[(C_5Me_5)Fe(C_5H_5)]$	+0.18 [e]		CH_2Cl_2	5
	+0.35		THF [f]	33
$[(C_5Bz_5)Fe(C_5H_5)]$	+0.39	82	CH_2Cl_2 [b]	[c]
$[(C_5H_4Bz)Fe(C_5H_5)]$	+0.35 [g]		MeCN	34
$[(C_5H_4Bz)_2Fe]$	+0.34 [g]		MeCN	34
$[(C_5H_5)_2Fe]$	+0.45	78	CH_2Cl_2 [b]	[c]
	+0.38	73	MeCN [d]	[c]
	+0.54	97	THF [b]	[c]

[a] Measured at 0.2 V s^{-1}. [b] $[NBu_4][ClO_4]$ (0.2 mol dm^{-3}). [c] Present work. [d] $[NEt_4][ClO_4]$ (0.2 mol dm^{-3}). [e] Converted to SCE. [f] $[NBu_4][BF_4]$ (0.1 mol dm^{-3}). [g] Referenced to the actual potential value for $[(C_5H_5)_2Fe]$.

The trend of ΔE_p with scan rate, which could give information on the extent of structural reorganization accompanying the redox change [27,28], departs appreciably from the constant value of 59 mV, theoretically expected for an electrochemically reversible one-electron step [26]. Nevertheless, possible uncompensated solution resistances do not allow us to infer unequivocally that this is attributable to the steric strains accompanying the oxidation of $[(C_5Bz_5)_2Fe]$ to $[(C_5Bz_5)_2Fe]^+$. In fact, under the same experimental conditions, the one-electron oxidation of ferrocene, which is known to involve minimal structural reorganization [29–32], exhibits a peak-to-peak separation increasing from 70 mV to 154 mV.

The pentabenzyl substituted species $[(C_5Bz_5)Fe(C_5H_5)]$ displays a cyclic voltammetric behaviour quite similar to that of $[(C_5Bz_5)_2Fe]$.

Table 1 summarizes the redox potentials for the one-electron oxidation of decabenzyl- and pentabenzylferrocenes and related molecules.

It is evident that substitution of the hydrogen atoms of ferrocene by the more electron-donating methyl or ethyl groups makes one-electron oxidation notably easier, whereas the electron-donating ability of the benzyl group is only slightly greater than that of the hydrogen atom.

2.2. Chemical oxidation of decabenzylferrocene

The synthesis of a decabenzylferrocenium salt was carried out by oxidation of decabenzylferrocene with silver hexafluorophosphate or with nitrosonium te-

trafluoroborate, at room temperature (eqns. (1) and (2)).

$$[(C_5Bz_5)_2Fe] + AgPF_6 \xrightarrow{C_6H_{12}} [(C_5Bz_5)_2Fe][PF_6] + Ag \quad (1)$$

$$[(C_5Bz_5)_2Fe] + NOBF_4 \xrightarrow{CH_2Cl_2} [(C_5Bz_5)_2Fe][BF_4] + NO \quad (2)$$

The reactions proceed in a very good yield (> 75%). Recrystallization from dichloromethane/diethyl ether gives the PF_6^- salt as dark-red to black cubic crystals and the BF_4^- salt as green crystals. Both compounds are air-stable. The intense colour of the PF_6^- compound is reminiscent of that of bis(tetraphenylcyclopentadienyl) iron(III) hexafluorophosphate [8].

NMR studies confirm the paramagnetic nature of the monocation compounds. In the ^1H NMR spectra, the signals are shifted downfield in comparison to the spectrum of the parent diamagnetic decabenzylferrocene. The methylene protons which are closest to the paramagnetic metal centre are the most affected; their signal is shifted by more than 12 ppm to lower field and broadened. In ^{13}C NMR spectra, only three signals are clearly visible, which we assign to the *ortho*, *meta*, and *para* carbon atoms of the phenyl rings. Signals for the remaining carbon centres (C_5-ring, methylene group, and quaternary phenyl carbon) could not be detected. They are apparently too broad and lost in the base line.

2.3. X-Ray crystal structure of $[(\eta^5\text{-}C_5Bz_5)_2Fe][BF_4]$

The crystal structure of $[(\eta^5\text{-}C_5Bz_5)_2Fe][BF_4]$ consists of decabenzylferrocenium cations and disordered tetrafluoroborate anions.

The $[PF_6]^-$ salt produced twinned crystals. Salts of $[TCNQ]^-$ or $[TCNE]^-$ anions, were not obtained because of the low oxidizing power of the cyanides towards $[(C_5Bz_5)_2Fe]$ (in CH_2Cl_2: $E^{\circ\prime}_{TCNQ/[TCNQ]^-} = +0.18$ V; $E^{\circ\prime}_{TCNE/[TCNE]^-} = +0.23$ V).

Figure 2 is an ORTEP plot of the structure of the decabenzylferrocenium cation. The structure of the cation $[(C_5Bz_5)_2Fe]^+$ is centrosymmetric with the iron atom lying on an inversion centre. Consequently the cyclopentadienyl rings assume a staggered conformation with exact D_{5d} symmetry as found for most decamethylferrocenium ions with different counteranions [15,17,19,21] and in the decaethylferrocenium cation [8,23]. The atomic coordinates are listed in Table 2.

As in the neutral precursor [24,25], the cyclopentadienyl rings are planar (within 0.03 Å) and the five phenyl groups, which are arranged in helical fashion, lie on the same side with respect to the cyclopentadienyl ring. The fact that in both the Fe^{II} and Fe^{III}

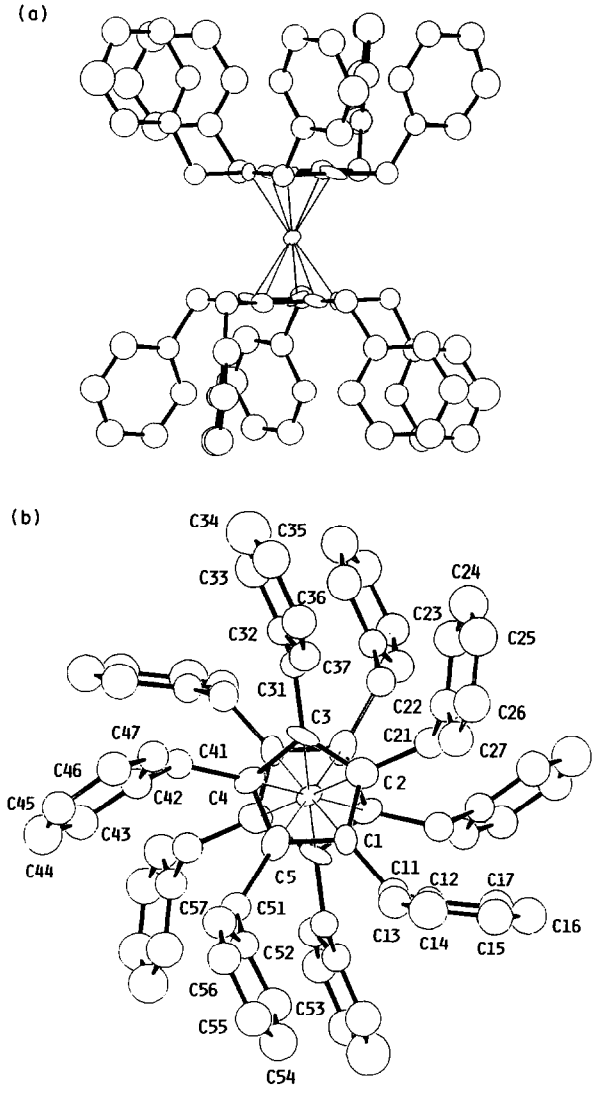

Fig. 2. ORTEP drawing of the cation $[(C_5Bz_5)_2Fe]^+$. (a) View parallel to the C_5-ring planes; (b) view perpendicular to the C_5-ring planes.

molecules, the benzyls maintain the same positions suggests that steric, rather than electronic, effects are responsible for the orientation. Different from the neutral precursor, where the methylene groups are tilted out of the plane of cyclopentadienyl rings, here the methylene groups are coplanar with them.

Table 3 reports a selection of bond distances and angles in the cation $[(C_5Bz_5)_2Fe]^+$, whereas Table 4 compares the most significant bond distances of the partners in the redox couple $[(C_5Bz_5)_2Fe]/[(C_5Bz_5)_2Fe]^+$ with those of closely related species. The data once again confirm that compared with neutral ferrocene molecules, in the ferrocenium cations the Fe–C and Fe–$C_{5(centroid)}$ distances are longer by about 0.05 Å.

TABLE 2. Fractional coordinates for $[(C_5Bz_5)_2Fe]^+$

Atom	x	y	z
Fe	0	0	0
C1	0.114(4)	0.054(5)	0.084(3)
C2	0.103(5)	−0.051(5)	0.089(4)
C3	0.127(4)	−0.093(4)	0.019(4)
C4	0.144(3)	−0.015(5)	−0.030(3)
C5	0.138(4)	0.075(5)	0.009(3)
C11	0.095(4)	0.125(4)	0.145(3)
C13	0.276(3)	0.131(3)	0.201(2)
C14	0.349(3)	0.133(3)	0.263(2)
C15	0.321(3)	0.128(3)	0.337(2)
C16	0.220(3)	0.122(3)	0.347(2)
C17	0.147(3)	0.120(3)	0.285(2)
C12	0.174(3)	0.125(3)	0.212(2)
C21	0.075(4)	−0.111(4)	0.156(3)
C23	0.151(2)	−0.278(3)	0.187(2)
C24	0.228(2)	−0.337(3)	0.222(2)
C25	0.311(2)	−0.294(3)	0.264(2)
C26	0.318(2)	−0.190(3)	0.269(2)
C27	0.241(2)	−0.130(3)	0.234(2)
C22	0.157(2)	−0.174(3)	0.193(2)
C31	0.125(4)	−0.199(4)	−0.004(3)
C33	0.239(3)	−0.341(3)	−0.034(2)
C34	0.327(3)	−0.397(3)	−0.021(2)
C35	0.405(3)	−0.365(3)	0.032(2)
C36	0.398(3)	−0.277(3)	0.073(2)
C37	0.307(3)	−0.221(3)	0.060(2)
C32	0.229(3)	−0.253(3)	0.006(2)
C41	0.171(3)	−0.024(4)	−0.110(2)
C43	0.294(2)	0.083(3)	−0.178(2)
C44	0.391(2)	0.107(3)	−0.193(2)
C45	0.474(2)	0.059(3)	−0.154(2)
C46	0.460(2)	−0.013(3)	−0.100(2)
C47	0.363(2)	−0.037(3)	−0.084(2)
C42	0.280(2)	0.011(3)	−0.123(2)
C51	0.154(4)	0.182(4)	−0.021(3)
C53	0.228(2)	0.322(3)	0.062(2)
C54	0.310(2)	0.375(3)	0.098(2)
C55	0.408(2)	0.341(3)	0.093(2)
C56	0.423(2)	0.254(3)	0.053(2)
C57	0.342(2)	0.202(3)	0.017(2)
C52	0.244(2)	0.235(3)	0.022(2)

TABLE 3. Bond distances (Å) and angles (°) in $[(C_5Bz_5)_2Fe]^+$

Fe–C1	2.14(6)	C3–C4	1.40(8)
Fe–C2	2.09(6)	C3–C31	1.47(7)
Fe–C3	2.10(6)	C4–C5	1.40(9)
Fe–C4	2.08(5)	C4–C41	1.50(7)
Fe–C5	2.09(6)	C5–C51	1.55(8)
$Fe–C_{5(cent)}$	1.71(5)	C11–C12	1.49(6)
C1–C2	1.42(9)	C21–C22	1.48(6)
C1–C5	1.44(8)	C31–C32	1.56(6)
C1–C11	1.48(9)	C41–C42	1.58(6)
C2–C3	1.42(9)	C51–C52	1.53(6)
C2–C21	1.51(9)		
C2–Fe–C3	39.7(2.5)	C1–C5–C4	109.1(5.4)
Fe–C1–C11	123.7(4.1)	C4–C5–C51	127.2(5.0)
C5–C1–C11	128.8(5.9)	C1–C5–C51	123.7(5.3)
C2–C1–C11	124.6(5.8)	Fe–C5–C51	124.9(3.8)
C2–C1–C5	106.4(5.9)	C1–C11–C12	114.4(4.6)
C1–C2–C21	127.4(5.9)	C2–C21–C22	114.6(4.5)
C1–C2–C3	107.7(5.9)	C21–C22–C23	119.4(3.6)
Fe–C2–C21	124.7(4.2)	C3–C31–C32	115.5(4.3)
C3–C2–C21	124.8(5.9)	C31–C32–C37	121.3(3.6)
C2–C3–C31	128.4(5.8)	C31–C32–C33	118.4(3.4)
C2–C3–C4	108.9(5.5)	C4–C41–C42	116.5(3.6)
Fe–C3–C31	122.6(4.1)	C41–C42–C47	118.9(3.3)
C4–C3–C31	122.4(5.5)	C41–C42–C43	120.9(3.2)
C3–C4–C41	127.7(5.4)	C5–C51–C52	113.3(4.2)
C3–C4–C5	107.6(4.7)	C51–C52–C57	120.6(3.7)
Fe–C4–C41	125.5(3.1)	C51–C52–C53	119.3(3.2)
C5–C4–C41	124.6(5.3)		

2.4. EPR measurements

X-Band EPR spectra of a powdered sample of the electrogenerated $[(C_5Bz_5)_2Fe]PF_6$, obtained by evaporating the solvent from a solution, have been recorded from 4.2 K to 300 K. Figure 3 shows the spectrum at liquid helium temperature.

A main feature centred at $g = 4.7$ is present together with a minor isotropic signal at $g = 2$. Since the intensity of this isotropic signal ($\Delta B_{pp} = 0.06$ T) tends

TABLE 4. Comparison of selected bond distances in $[(C_5R_5)_2Fe]^{0,+}$ redox couples

	Fe–C (Å)	C–C (Å)	$Fe–C_{5(cent)}$ (Å)	$C–C_R$ (Å)	CP rings conformation	Ref.
$[(C_5Bz_5)_2Fe]$	2.06	1.43	1.66	1.51	Staggered	24,25
$[(C_5Bz_5)_2Fe]^+$ [a]	2.10	1.42	1.71	1.50	Staggered	b
$[(C_5Me_5)_2Fe]$	2.05	1.42	1.66	1.50	Staggered	11
$[(C_5Me_5)_2Fe]^+$ [c]	2.10	1.42	1.69	1.51	Staggered	16
$[(C_5Me_5)_2Fe]^+$ [d]	2.10	1.42	1.71	1.50	Eclipsed	20
$[(C_5Et_5)_2Fe]^+$ [c]	2.09	1.43	1.70	1.50	Staggered	9
$[(C_5H_5)_2Fe]$	2.03	1.39	1.66		Disordered	29
$[(C_5H_5)_2Fe]^+$ [e]	2.05	1.34	1.70		Staggered	32

[a] $[BF_4]^-$ counteranion. [b] Present paper. [c] $[TCNQ]^-$ counteranion. [d] $[Br_3]^-$ counteranion. [e] $[PF_6]^-$ counteranion.

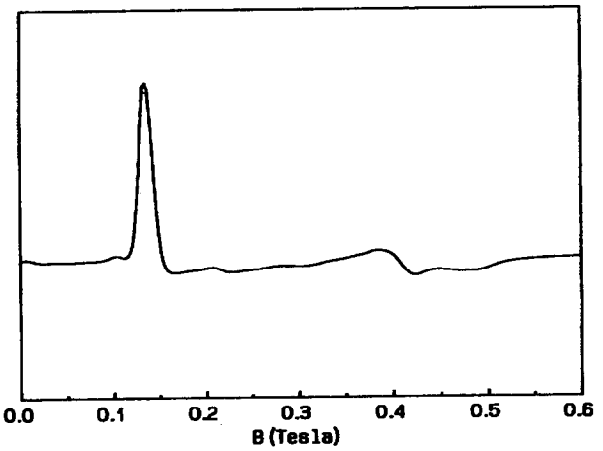

Fig. 3. X-Band EPR spectrum recorded at 4.2 K of a dichloromethane solution of $[(C_5Bz_5)_2Fe]^+$.

to increase slightly with the age of the sample, we attribute it to minor decomposition.

The shape and position of the main peak are consistent with the $g_{\parallel}$ values of ferrocenium species. The lack of the corresponding $g_{\perp}$, presumably due to the signal broadening by field effects, is not new, in that it was previously reported for $[(C_5Et_5)_2Fe]^+$ [9].

As summarized in Table 5, the cation $[(C_5Bz_5)_2Fe]^+$ possesses the highest $g_{\parallel}$ value of all ferrocenium complexes. According to Prins [37], this is related to the fact that electron removal causes the least distortion from high symmetry.

3. Materials and apparatus

The preparation of $[(C_5Bz_5)_2Fe]$ [24,25] and $[(C_5Bz_5)Fe(C_5H_5)]$ [25] has been previously described. $[(\eta^5\text{-}C_5H_5)_2Fe][PF_6]$ was an Aldrich product.

$[(\eta^5\text{-}C_5Bz_5)_2Fe][BF_4]$. 0.90 g (0.83 mmol) of $[(\eta^5\text{-}C_5Bz_5)_2Fe]$ were dissolved in 20 ml of CH_2Cl_2 and 0.14 g (1.20 mmol) of $NOBF_4$ were added. The yellow solution immediately turns green and gas is evolved. After 1 h, the green-brown solution was decanted from unreacted $NOBF_4$, it was layered with 20 ml of diethyl ether and was cooled to +2°C. Green crystals separated from the solution (0.75 g, 77%).

The IR spectrum exhibits the bands of the parent metallocene plus a strong split signal at 1051 and 1080 cm^{-1} ($\nu_3(BF_4^-)$) [38]. ^1H NMR (CD_2Cl_2) [39*]: δ 10.83, 11.33 (s, 50 H, phenyl), 16.3 (s, 20 H, CH_2, $w_{1/2} = 310$ Hz) ppm. ^{13}C NMR (CD_2Cl_2) [39*]: δ 130.57, 135.14, 137.97 (broad) ppm.

$[(\eta^5\text{-}C_5Bz_5)_2Fe][PF_6]$. 35 ml of cyclohexane were added to a mixture of $[(C_5Bz_5)_2Fe]$ (0.53 g, 0.49 mmol) and $AgPF_6$ (0.13 g, 0.50 mmol). The yellow slurry was stirred for 24 h in the dark. The resulting black-brown precipitate was filtered and was extracted with CH_2Cl_2, yielding a black-green solution, which was layered with 5 ml of diethyl ether and cooled to +2°C, leading to dark red-to-black crystals of $[(C_5Bz_5)_2Fe][PF_6]$.

The IR spectrum exhibits the bands of the parent metallocene plus a very strong split signal at 831 and 853 cm^{-1} ($\nu_3(PF_6^-)$) with shoulders at 877 and 908 cm^{-1} and a medium band at 557 cm^{-1} ($\nu_4(PF_6^-)$) [38]. ^1H NMR (CD_2Cl_2) [39*]: δ 10.87, 11.37 (s, 50 H, phenyl), 16.20 (s, 20 H, CH_2, $w_{1/2} = 340$ Hz) ppm. ^{13}C NMR (CD_2Cl_2) [39]: δ 130.67, 135.35, 137.71 (broad) ppm.

3.1. X-Ray analysis

A green-brown parallelopiped crystal of $[(\eta^5\text{-}C_5H_5)_2Fe][BF_4]$ was mounted on an Enraf-Nonius CAD4 diffractometer. A summary of the crystallographic data is reported in Table 6. Unit cell dimensions were determined from the angular settings of 22 carefully centered reflections with $8 < \theta < 15$. Intensity data for 6010 independent reflections having $\theta < 25$ were collected in the ranges $-15 < h < 15$, $0 < k < 15$, $0 < l < 21$. Intensities were corrected for Lorentz and polarization effects. The intensities of three control reflections were monitored periodically and did not show any significant variation during data collection.

The systematic absences in the diffraction data suggested the centrosymmetric space group $P2_1/c$, but the distribution of the E values was ambiguous being centric at $\sin(\theta)/\lambda < 0.42$ and acentric above this value. Consequently, the acentric space group $P2_1$ could not be rejected. It was also supported by the fact that only two molecules are present in the unit cell. This means that in the space group $P2_1/c$, the two molecules must be in the special positions of multiplicity, two located on a centre of symmetry. However, only the ferrocenium cation can have centrosymmetric local symmetry, the BF_4^- anion being tetrahedral. Hence, either the

TABLE 5. Low-temperature EPR data on selected metallocenium ions

Complex	$g_{\parallel}$	$g_{\perp}$	Ref.
$[(C_5H_4\text{-}(CH_2)_3\text{-}C_5H_4)Fe]^+$ [a]	3.86	1.81	35
$[(C_5H_4Me)_2Fe]^+$ [a]	4.00	1.92	35
$[(C_5H_5)_2Fe]^+$ [a]	4.60	1.95	Present paper
$[(C_5Me_5)_2Fe]^+$ [a]	4.43	1.35	35
$[(C_5Bz_5)_2Fe]^+$ [a]	4.7	–	Present paper
$[(C_5Et_5)_2Fe]^+$ [a]	4.59	–	9
$[(C_5Me_5)_2Os]^+$ [b]	5.27	1.99	36

[a] $[PF_6]^-$ counteranion. [b] $[BF_4]^-$ counteranion.

* Reference number with asterisk indicates a note in the list of references.

TABLE 6. Crystal data and summary of intensity data collection and structure refinement for $[(C_5Bz_5)_2Fe][BF_4]$

Colour/shape	Green-brown/parallelepiped
FW	1174.1
Space group	$P2_1/c$
Temperature (°C)	22
a (Å)	13.403(5)
b (Å)	13.398(2)
c (Å)	17.771(3)
β (°)	96.66(2)
Cell volume (Å^3)	3169.7
Z	2
D_{calcd} (g cm^{-3})	1.23
μ_{calcd} (cm^{-1})	2.9
Diffractometer/scan	Enraf-Nonius CAD4/θ–2θ
Transmission range (%)	98–100
Radiation, graphite monochromator	Mo Kα (λ = 0.71073 Å)
Crystal dimensions (mm)	0.18×0.22×0.25
Scan width	1.0+0.35 tan (θ)
Standard reflections	042, 200, 411
Decay of standards	Not observed
Reflections measured	6010
Range (°)	$2 < \theta < 25$
Reflections observed $I > 3\sigma(I)$	1373
Computer program [40]	SHELX76
Structure solution	Heavy-atom techniques
No. of parameters varied	108
Weights	Unit
R [a]	0.102
R_w [b]	0.102

[a] $R = \Sigma[|F_o| - |F_c|]/\Sigma|F_o|$.
[b] $R_w = \{\Sigma w[|F_o| - |F_c|]^2\}/\{\Sigma w|F_o|^2\}^{1/2}$.

space group is the acentric $P2_1$ with the two molecules in general positions or the tetrafluoroborate anion is disordered over two positions with 50% occupancy. The structure of the cation may be solved in the $P2_1/c$ space group, but the BF_4^- anion appeared so greatly disordered that the diffuse electron density could not be fitted. However, attempts to locate the anion in the space group $P2_1$ failed because the Fourier difference maps phased on a partial structure of the ferricinium cation did not show the anion and the strong correlations among the parameters prevented any refinement and improvement of phases. The boron atoms should lie on the centre of symmetry at 0, $\frac{1}{2}$, 0 in $P2_1/c$, but because of the poor resolution, and because the main goal of the diffraction experiment was the structural determination of the ferricinium cation we decided to perform the refinement in the centric space group leaving the anion undetermined.

The refinement was performed in the space group $P2_1/c$ by means of the full matrix least-squares method using 1373 reflections having $I > 3\sigma$ (I). Anisotropic thermal parameters were refined for the iron atom only, the phenyl rings were treated as rigid groups and the hydrogen atoms were introduced in calculated positions in the last cycles of the refinement. All calculations were performed on an IBM RISC 330 computer using the SHELX76 program [40]. Table 2 reports the list of the final atomic coordinates for non-hydrogen atoms with estimated standard deviations from the least-squares inverse matrix. The molecular plots were produced by the program ORTEP [41]. Full lists of bond lengths and angles are available from the Cambridge Crystallographic Data Centre.

3.2. Electrochemistry

Materials and apparatus for electrochemistry have been described in the first paper of the series [42].

References

1 P. Zanello, G. Opromolla, G. Giorgi, J.C. van de Grampel and H.F.M. Schoo, *Polyhedron, 12* (1993) 1329.
2 W.E. Geiger, *J. Organomet. Chem. Libr., 22* (1990) 142.
3 U. Koelle and F. Khouzami, *Angew. Chem., Int. Ed. Engl., 19* (1980) 640.
4 J.L. Robbins, N. Eldenstein, B. Spencer and J.C. Smart, *J. Am. Chem. Soc., 104* (1982) 1882.
5 P.G. Gassman, D.W. Macomber and J.W. Hershberger, *Organometallics, 2* (1983) 1470.
6 T. Gennett, D.F. Milner and M.J. Weaver, *J. Phys. Chem., 89* (1985) 2787.
7 W.E. Britton, R. Kashyap, M.E.-Hashash and M.E.-Kady, *Organometallics, 5* (1986) 1029.
8 M.P. Castellani, J.M. Wright, S.J. Geib, A.L. Rheingold and W.C. Trogler, *Organometallics, 5* (1986) 1116.
9 K.-M. Chi, J.C. Calabrese, W.M. Reiff and J.S. Miller, *Organometallics, 10* (1991) 688.
10 Y.T. Struchkov, V.G. Andrianov, T.N. Sal'nikova, I.R. Lyatifov and R.B. Materikova, *J. Organomet. Chem., 145* (1978) 213.
11 D.P. Freyberg, J.L. Robbins, K.N. Raymond and J.C. Smart, *J. Am. Chem. Soc., 101* (1979) 892.
12 A. Almenningen, A. Haaland, S. Samdal, J. Brunvoll, J.L. Robbins and J.C. Smart, *J. Organomet. Chem., 173* (1979) 293.
13 E. Gebert, A.H. Reis, Jr., J.S. Miller, H. Rommelmann and A.J. Epstein, *J. Am. Chem. Soc., 104* (1982) 4403.
14 D.A. Dixon, J.C. Calabrese and J.S. Miller, *J. Am. Chem. Soc., 108* (1986) 2582.
15 J.S. Miller, J.C. Calabrese, H. Rommelmann, S.R. Chittipeddi, J.H. Zhang, W.M. Reiff and A.J. Epstein, *J. Am. Chem. Soc., 109* (1987) 769.
16 J.S. Miller, J.H. Zhang, W.M. Reiff, D.A. Dixon, L.D. Preston, A.H. Reis, Jr., E. Gebert, M. Extine, J. Troup, A.J. Epstein and M.D. Ward, *J. Phys. Chem., 91* (1987) 4344.
17 J.S. Miller, J.H. Zhang and W.M. Reiff, *J. Am. Chem. Soc., 109* (1987) 4584.
18 J.S. Miller, J.C. Calabrese and A.J. Epstein, *Inorg. Chem., 28* (1989) 4230.
19 J.S. Miller, M.D. Ward, J.H. Zhang and W.M. Reiff, *Inorg. Chem., 29* (1990) 4063.
20 J. Pickardt, H. Schumann and R. Mohtachemi, *Acta Crystallogr., Sect. C, 46* (1990) 39.
21 J.S. Miller, J.C. Calabrese, R.L. Harlow, D.A. Dixon, J.H. Zhang, W.M. Reiff, S. Chittipeddi, M.A. Selover and A.J. Epstein, *J. Am. Chem. Soc., 112* (1990) 5496.

22 G. Matsubayashi and A. Yokozawa, *Inorg. Chim. Acta, 193* (1992) 137.
23 D. Stein, H. Sitzmann, R. Boese, E. Dormann and H. Winter, *J. Organomet. Chem., 412* (1991) 143.
24 H. Schumann, C. Janiak, R.D. Köhn, J. Loebel and A. Dietrich, *J. Organomet. Chem., 365* (1989) 137.
25 M.D. Rausch, W.-M. Tsai, J.W. Chambers, R.D. Rogers and H.G. Alt, *Organometallics, 8* (1989) 816.
26 E.R. Brown and J.R. Sandifer, in B.W. Rossiter and J.F. Hamilton (eds.), *Physical Methods of Chemistry. Electrochemical Methods*, Vol. II, Wiley, New York, 1986, Ch. IV.
27 P. Zanello, in I. Bernal (ed.), *Stereochemistry of Organometallic and Inorganic Compounds*, Vol. IV, Elsevier, Amsterdam, 1990, p. 181.
28 P. Zanello, *Struct. Bonding (Berlin), 79* (1992) 101.
29 P. Seiler and J.D. Dunitz, *Acta Crystallogr., Sect. B, 35* (1979) 1068.
30 M.R. Churchill, A.G. Lander and A.L. Rheingold, *Inorg. Chem., 20* (1981) 849.
31 S.J. Geib, A.L. Rheingold, T.Y. Dong and D.N. Hendrickson, *J. Organomet. Chem., 312* (1986) 241.
32 R. Martinez and A. Tiripicchio, *Acta Crystallogr., Sect. C, 46* (1990) 202.
33 S. Rittinger, D. Buchholz, M.-H. Delville-Desbois, J. Linares, F. Varret, R. Boese, L. Zsolnai, G. Huttner and D. Astruc, *Organometallics, 11* (1992) 1454.
34 G.L.K. Hoh, W.E. McEwen and J. Kleinberg, *J. Am. Chem. Soc., 83* (1961) 3949.
35 D.M. Duggan and D.N. Hendrickson, *Inorg. Chem., 14* (1975) 955.
36 D. O'Hare, J.C. Green, T.P. Chadwick and J.S. Miller, *Organometallics, 7* (1988) 1335.
37 R. Prins, *Mol. Phys., 19* (1970) 603.
38 H. Siebert, *Anwendungen der Schwingungsspektroskopie in der Anorganischen Chemie*, Springer-Verlag, Berlin, 1966.
39 Bruker WP 80SY, 80 MHz for ^{1}H, 20.15 MHz for ^{13}C; chemical shifts are given in the δ-scale against a TMS reference. The shifts were measured with respect to dichloromethane (5.32 or 53.80 ppm).
40 G.M. Sheldrick, *SHELX76: Program for Crystal Structure Determination*, University of Cambridge, Cambridge, 1976.
41 C.K. Johnson, *ORTEP: ORNL Report No. 3794*, Oak Ridge National Laboratory, Oak Ridge, TN, 1971.
42 P. Zanello, G. Opromolla, M. Casarin, M. Herberhold and P. Leitner, *J. Organomet. Chem., 443* (1993) 199.